Available online at www.sciencedirect.com

ScienceDirect

*Mendeleev Commun.*, 2021, **31**, 221–223

Mendeleev Communications

# Tuning the morphology and magnetic properties of single-domain $SrFe_8Al_4O_{19}$ particles prepared by a citrate auto-combustion method

**Anastasia E. Sleptsova,[a] Liudmila N. Alyabyeva,[b] Evgeny A. Gorbachev,*[a,c] Ekaterina S. Kozlyakova,[d] Maxim A. Karpov,[a] Chen Xinming,[c] Alexander V. Vasiliev,[a] Boris P. Gorshunov,[b] Anatoly S. Prokhorov,[b,e] Pavel E. Kazin[a] and Lev A. Trusov[a,c]**

[a] *Department of Chemistry, M. V. Lomonosov Moscow State University, 119991 Moscow, Russian Federation. E-mail: ev.a.gorbachev@gmail.com*
[b] *Moscow Institute of Physics and Technology, 141701 Dolgoprudny, Moscow Region, Russian Federation*
[c] *MSU-BIT University, 517182 Shenzhen, China*
[d] *Department of Physics, M. V. Lomonosov Moscow State University, 119991 Moscow, Russian Federation*
[e] *A. M. Prokhorov General Physics Institute, Russian Academy of Sciences, 119991 Moscow, Russian Federation*

DOI: 10.1016/j.mencom.2021.03.025

**Single-domain particles of $SrFe_8Al_4O_{19}$ were prepared by thermal treatment of porous products of citrate–nitrate auto-combustion at 1200 °C, and the effect of synthesis time on the particle morphology and magnetic properties was estimated. The procedure allows one to obtain $SrFe_8Al_4O_{19}$ particles with mean diameters of 100–460 nm and coercivity ranges from 14.5 to 18.4 kOe, while ferromagnetic resonance frequencies vary from 149 to 164 GHz.**

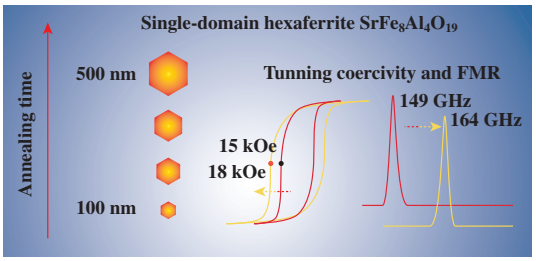


*Keywords*: hexaferrites, ferrites, magnetic materials, permanent magnets, high coercivity, ferromagnetic resonance.

Although M-type hexaferrites ($BaFe_{12}O_{19}$ and $SrFe_{12}O_{19}$) are well-studied compounds, they are still of great interest due to a unique set of finely tunable functional properties.[1] Large magneto-crystalline anisotropy and high coercivity form the basis for their wide applications as permanent magnets,[2] and high thermal and chemical stability makes it possible to produce nanomagnets for magnetic recording media,[3–5] fast-response magnetoactive colloids[6,7] and hard magnetic cores of exchange-coupled nano-composites.[8,9] Moreover, the hexaferrites display specific millimeter-wave (sub-THz) absorption due to ferromagnetic resonance (FMR), which is essential for modern wireless communication technologies.[10–13] The properties of the hexaferrites are extremely sensitive to particle morphology and ionic substitutions in their crystal structure.

Recently, we presented a method for manufacturing highly aluminum substituted strontium hexaferrite in the form of single-domain particles.[13,14] This resulted in hexaferrite materials with giant coercivity up to 40 kOe and record-high natural FMR (under zero magnetic field) frequencies of 160–250 GHz. This simple method is based on the heat treatment of porous oxide precursors obtained by a citrate auto-combustion method. Nevertheless, it implies the possibility to modify the morphology and functional properties of particles by varying heat treatment parameters.

We studied the influence of the time of annealing at 1200 °C on the morphology, magnetic properties and millimeter-wave absorption of $SrFe_8Al_4O_{19}$ particles.

The M-type $SrFe_8Al_4O_{19}$ hexaferrite particles were produced by a citrate method described previously.[14] Briefly, strontium, iron and aluminum nitrates and citric acid (all of high purity grade from Sigma-Aldrich) were mixed in an aqueous solution to obtain a molar ratio of 1 : 3 between metal and citrate ions. The solution was neutralized with $NH_3$(aq.) and then dehydrated by heating in a sand bath. The product was spontaneously combusted to form a highly porous precursor powder. The powder was heated to 1200 °C with a rate of 10 K $min^{-1}$ and exposed at this temperature for 0, 0.5, 2, 8, 14 and 24 h.

According to X-ray diffraction data (Rigaku D-Max 2500, CuKα radiation), the samples contained a single crystalline M-type hexaferrite phase. The lattice parameters of the hexaferrite samples exposed for 0 h were slightly larger than those of the samples exposed for longer times (Table 1); thus, the Al substitution was not fully completed. The hexaferrite composition estimated from the lattice parameters is $SrFe_{8.15}Al_{3.85}O_{19}$.[14] The parameters of the samples exposed for 0.5 h and longer are in a good agreement with previously reported data for a $SrFe_8Al_4O_{19}$ phase.[14]

The particle morphology [Figures 1(*a*)–(*c*), Table 1] was determined by scanning electron microscopy (Carl Zeiss NVision40). The particles had a thick-plate shape with wide diameter distributions [Figure 1(*d*)]. The mean particle diameter increased from 100 to 460 nm as the exposure time was increased from 0 to 24 h. The single-domain limit of $SrFe_8Al_4O_{19}$ was estimated at 8 μm;[13,15] therefore, the particles within the samples mainly occurred in a single-domain state.

Figure 2 shows the magnetic hysteresis loops of the samples (Quantum Design PPMS, magnetic fields up to 6 T) and Table 1 summarizes the corresponding properties. The shapes of the hysteresis loops are typical of randomly oriented single-domain Stoner–Wohlfarth particles with $M_r/M_S$ close to 0.5.[16] The replacement of paramagnetic iron ions by diamagnetic aluminum in hexaferrite results in a gradual decrease of saturation magnetization $M_S$[1,17,18], while the coercivity rises only for single-domain particles.[14]

**Table 1** Unit cell parameters (*a*, *c*), aluminum content *x* estimated from the lattice parameters, mean particle diameter $d_{mean}$, magnetic properties (coercive field $H_C$, saturation magnetization $M_S$ at 60 kOe, and remanence $M_r$), and natural ferromagnetic resonance frequency $f_r$ of the samples.

| Exposure time/h | *x* | *a*/Å | *c*/Å | $d_{mean}$/nm | $H_C$/kOe | $M_S$/emu g$^{-1}$ | $M_r$/emu g$^{-1}$ | $M_r/M_S$ | $f_r$/GHz |
|---|---|---|---|---|---|---|---|---|---|
| 0.0 | 3.85 | 5.7905(1) | 22.7459(7) | 100 | 14.5 | 14.0 | 7.5 | 0.51 | 149 |
| 0.5 | 3.95 | 5.7886(1) | 22.7330(7) | 150 | 15.3 | 13.4 | 7.3 | 0.52 | 155 |
| 2.0 | 4.00 | 5.7880(1) | 22.7311(4) | 230 | 15.6 | 13.5 | 7.3 | 0.52 | 164 |
| 8.0 | 4.00 | 5.7874(1) | 22.7283(5) | 260 | 15.9 | 13.5 | 7.4 | 0.53 | 164 |
| 14.0 | 4.00 | 5.7879(1) | 22.7277(5) | 280 | 16.8 | 13.4 | 7.1 | 0.51 | 164 |
| 24.0 | 4.00 | 5.7878(1) | 22.7280(4) | 460 | 18.4 | 13.6 | 7.3 | 0.51 | 164 |

The saturation magnetization $M_S$ of the samples annealed for 0.5–24 h was close to that reported previously for $SrFe_8Al_4O_{19}$.[14] The 0 h sample had higher $M_S$, which indicates lower Al substitution and is consistent with XRD analysis data. The coercivity $H_C$ sharply jumped up as the exposure time was increased from 0 to 2 h because of higher aluminum substitution. For annealing times of 2–24 h, the coercivity gradually raised from 15.6 to 18.4 kOe. It is well known that $Al^{3+}$ ions substitute for iron ones in octahedral 12k and 2a sites, whose magnetic moments are co-directional with that of the hexaferrite unit cell.[14,19] Furthermore, $Fe^{3+}$ ions in these sublattices contribute weakly to the magneto-crystalline anisotropy constant $K_1$.[20] Therefore, aluminum incorporation into the hexaferrite crystal lattice slightly decreased $K_1$ but considerably reduced the $M_S$ of the material,[21] which led to a significant increase in $H_C$ according to the Stoner–Wohlfarth model ($H_C \sim K_1/M_S$).[16] As a result, the coercivity of all the samples was much higher than the largest reported for unsubstituted hexaferrites (not higher than 7 kOe[2]). The coercivity of nano- and submicron particles is also strongly affected by particle size effects.[1,2,22] Small particles with diameters of <10 nm are super-paramagnetic with $H_C = 0$ Oe; however, the coercivity of larger particles was reduced by thermal demagnetization.[2,22] Thus, the observed increase in the coercivity was due to continuous recrystallization resulting in particle enlargement.

The room temperature FMR spectra of the samples (composite pellets of PMMA/hexaferrite powder (1 : 9, by weight) fabricated by hot pressing as described previously[13]) were recorded with a terahertz time-domain spectrometer Teraview TPS 3000 in the absence of an external magnetic field. The samples possessed FMR frequencies at 149 GHz for 0 h, 155 GHz for 0.5 h and 164 GHz for the rest of exposure times resulting in similar values for $MFe_8Al_4O_{19}$.[13] The value of $f_r$ is sensitive only to hexaferrite composition, while particle size does not affect it. This could be explained by the fact that the magnetic anisotropy constant and the saturation magnetization do almost not depend on hexaferrite particle size in a sub-micron range (100–1000 nm) since the surface contribution is low in this case.[22] In addition, the shape

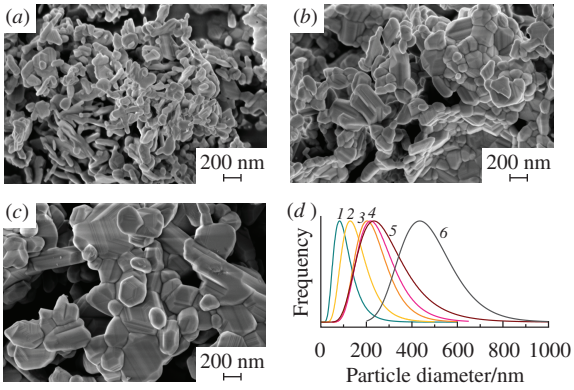


**Figure 1** (*a*)–(*c*) SEM images of hexaferrite powders obtained at 1200 °C with exposure times of 0, 0.5 and 14 h, respectively; (*d*) lognormal distributions of particle diameters calculated by fitting histograms with exposure times of (*1*) 0, (*2*) 0.5, (*3*) 2, (*4*) 8, (5) 14 and (*6*) 24 h.

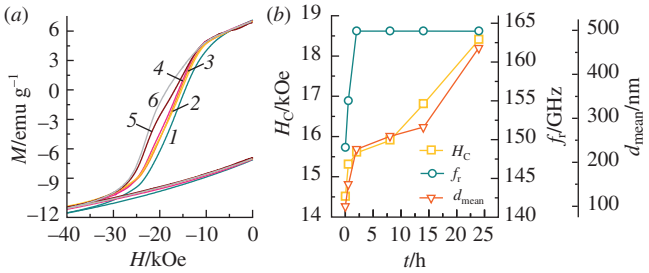


**Figure 2** (*a*) Magnetic hysteresis loops; (*b*) dependences of coercivity ($H_C$), ferromagnetic resonance frequency ($f_r$) and mean particle diameter ($d_{mean}$) on exposure time at 1200 °C.

of particles has no effect on $f_r$ due to their low magnetization and, consequently, the negligible demagnetization field $H_d = 4\pi\rho M_S$ (where $\rho \approx 4.7$ g cm$^{-3}$ is the crystallographic density of hexaferrite) compared to the anisotropy field $H_a$ (in our case, $H_d \approx 0.9$ kOe and $H_a \approx 40$ kOe[13]). Thus, according to the Kittel formula[23] $f_r \sim H_a = 2K_1/M_S$, the ferromagnetic resonance frequency is affected only by the aluminum content of the hexaferrite lattice.

The difference in behaviors of $H_C$ and $f_r$ with particle size is caused by different relationships of these properties to thermal fluctuation of particle magnetization. The probability of a particle with a certain volume to be spontaneously demagnetized increases with a decrease in the particle size,[22] which leads to a decrease in the coercivity of the particle ensemble, while it does not affect the average values of $H_a$ and $f_r$.

Thus, we studied the formation of single-phase $SrFe_8Al_4O_{19}$ hexaferrite by annealing porous products obtained by the auto-combustion of citrate solutions. This method offers a promising way to prepare highly substituted hexaferrite particles with tunable sizes and high magnetic and millimeter-wave absorption properties. The highest reported coercivity of nanosized hexaferrite particles was 14.5 kOe. It was also found that the mean particle diameter in a range of 230–460 nm does not affect the ferromagnetic resonance frequency of the $SrFe_8Al_4O_{19}$ hexaferrites (164 GHz); however, it has a strong effect on their coercivity, which increases from 15.3 to 18.4 kOe, respectively. The hexaferrite powders with high phase purity and tunable particle size within the single-domain region are essential for the production of fine-grained ceramics, hard magnetic films, coatings, and composites. Due to their high-frequency absorption properties and high magnetic hardness, the developed hexaferrite materials are promising for modern applications, such as spintronics, electromagnetic shielding, durable magnetic recording, and the next generation of wireless technologies.

This work was supported by the Russian Foundation for Basic Research (grant no. 20-02-00887). SEM measurements were performed using the equipment of the JRC PMR IGIC RAS.

## References

1 H. Kojima, in *Handbook of Magnetic Materials*, ed. E. P. Wohlfarth, North-Holland Publishing Company, Amsterdam, 1982, vol. 3, pp. 305–391.
2 R. C. Pullar, *Prog. Mater. Sci.*, 2012, **57**, 1191.

3 O. Shimizu, M. Oyanagi, A. Morooka, M. Mori, Y. Kurihashi, T. Tada, H. Suzuki and T. Harasawa, *J. Magn. Magn. Mater.*, 2016, **400**, 365.
4 N. Nagai, N. Sugita and M. Maekawa, *J. Magn. Magn. Mater.*, 1993, **120**, 33.
5 M. R. Lukatskaya, L. A. Trusov, A. A. Eliseev, A. V. Lukashin, M. Jansen, P. E. Kazin and K. S. Napolskii, *Chem. Commun.*, 2011, **47**, 2396.
6 L. A. Trusov, A. V. Vasiliev, M. R. Lukatskaya, D. D. Zaytsev, M. Jansen and P. E. Kazin, *Chem. Commun.*, 2014, **50**, 14581.
7 A. A. Eliseev, A. A. Eliseev, L. A. Trusov, A. P. Chumakov, P. Boesecke, E. O. Anokhin, A. V. Vasiliev, A. E. Sleptsova, E. A. Gorbachev, V. V. Korolev and P. E. Kazin, *Appl. Phys. Lett.*, 2018, **113**, 113106.
8 E. A. Gorbachev, L. A. Trusov, A. E. Sleptsova, E. O. Anokhin, D. D. Zaitsev, A. V. Vasiliev, A. A. Eliseev and P. E. Kazin, *Mendeleev Commun.*, 2018, **28**, 401.
9 G. Han, Y. Liu, W. Yang, S. Geng, W. Cui and Y. Yu, *Nanoscale*, 2019, **11**, 10629.
10 V. G. Harris, Z. Chen, Y. Chen, S. Yoon, T. Sakai, A. Gieler, A. Yang and Y. He, *J. Appl. Phys.*, 2006, **99**, 08M911.
11 V. G. Harris, A. Geiler, Y. Chen, S. D. Yoon, M. Wu, A. Yang, Z. Chen, P. He, P. V. Parimi, X. Zuo, C. E. Patton, M. Abe, O. Acher and C. Vittoria, *J. Magn. Magn. Mater.*, 2009, **321**, 2035.
12 Y. Chen, T. Sakai, T. Chen, S. D. Yoon, A. L. Geiler, C. Vittoria and V. G. Harris, *Appl. Phys. Lett.*, 2006, **88**, 062516.
13 E. A. Gorbachev, L. A. Trusov, A. E. Sleptsova, E. S. Kozlyakova, L. N. Alyabyeva, S. R. Yegiyan, A. S. Prokhorov, V. A. Lebedev, I. V. Roslyakov, A. V. Vasiliev and P. E. Kazin, *Mater. Today*, 2020, **32**, 13.
14 L. A. Trusov, E. A. Gorbachev, V. A. Lebedev, A. E. Sleptsova, I. V. Roslyakov, E. S. Kozlyakova, A. V. Vasiliev, R. E. Dinnebier, M. Jansen and P. E. Kazin, *Chem. Commun.*, 2018, **54**, 479.
15 J. N. Dahal, L. Wang, S. R. Mishra, V. V. Nguyen and J. P. Liu, *J. Alloys Compd.*, 2014, **595**, 213.
16 E. C. Stoner and E. P. Wohlfarth, *Philos. Trans. R. Soc., A*, 1948, **240**, 599.
17 P. E. Kazin, L. A. Trusov, D. D. Zaitsev, Y. D. Tretyakov and M. Jansen, *J. Magn. Magn. Mater.*, 2008, **320**, 1068.
18 H. Luo, B. K. Rai, S. R. Mishra, V. V. Nguyen and J. P. Liu, *J. Magn. Magn. Mater.*, 2012, **324**, 2602.
19 F. Sandiumenge, S. Gali and J. Rodriguez, *Mater. Res. Bull.*, 1988, **23**, 685.
20 Y. Xu, G. L. Yang, D. P. Chu and H. R. Zhai, *Phys. Status Solidi*, 1990, **157**, 685.
21 D. J. De Bitetto, *J. Appl. Phys.*, 1964, **35**, 3482.
22 B. T. Shirk and W. R. Buessem, *IEEE Trans. Magn.*, 1971, **7**, 659.
23 C. Kittel, *Phys. Rev.*, 1948, **73**, 155.

*Received: 13th November 2020; Com. 20/6366*